Mechanical Properties of Amorphous Silicon Nanoparticles

Dimitrios Kilymis, Céline Gérard, Laurent Pizzagalli

Mechanical properties of amorphous silicon nanoparticles

D. Kilymis and C. Gérard and L. Pizzagalli

Abstract The compression of amorphous silicon nanoparticles is investigated by means of molecular dynamics simulations, at two temperatures and for diameters equal to 16 nm and 34 nm. The nanoparticles deform plastically, with maximum contact stresses in the range 8.5–11 GPa, corresponding to strains between 12% and 24%. No clear size effect is observed. Despite large contact stress values, the formation of high density crystalline or amorphous phases is not observed, presumably due to the presence of lateral free surfaces allowing for plasticity deconfinement. Atomic displacements analysis confirms that during plastic deformation, atoms close to indenters are first pushed towards the nanoparticle center, before migrating laterally towards free surfaces. Plastic deformation leads to an increase of fivefold coordinated atoms, which are spatially correlated with the largest atomic displacements.

Key words: Nanoparticles, Amorphous silicon, Molecular dynamics, Plasticity

D. Kilymis
CIRIMAT - UMR CNRS 5085, Université Toulouse 3 - Paul Sabatier, Bâtiment CIRIMAT, 118 Route de Narbonne, 31062 Toulouse cedex 9, France, e-mail: kilymis@chimie.ups-tlse.fr

C. Gérard
Institut Pprime, Université de Poitiers - CNRS - ISAE-ENSMA, F86962 Chasseneuil Futuroscope Cedex, France, e-mail: celine.gerard@ensma.fr

L. Pizzagalli
Institut Pprime, Université de Poitiers - CNRS - ISAE-ENSMA, SP2MI, Boulevard Marie et Pierre Curie, TSA 41123, 86073 Poitiers Cedex 9, France, e-mail: laurent.pizzagalli@univ-poitiers.fr

1 Introduction

Silicon nanoparticles (SiNP) can be used in many different domains, due to a combination of several outstanding properties. In particular possible applications concern electronics, photonics, plasmonics, as well as cell biology [1]. SiNP have also been shown to be potential candidates for new generation of Li ion batteries [2, 3]. Properties of SiNP can be tuned in many different ways, for instance by changing their size, functionalizing their surfaces and also by being included into larger structures where they can form superlattices. In addition to being abundant and cheap, silicon is the core of electronic technology, which obviously facilitates the integration of SiNP. Finally, it is also considered a model covalent material.

Some aspects of SiNP have already been extensively studied, in particular quantum confinement effects that greatly change the electronic structure at the nanometer scale [4]. However many other properties are expected to change as a function of size, not only because of quantum confinement, but also due to the large surface to volume ratio. For instance, it is known that there is a spectacular effect on the mechanical behavior when dimensions are reduced [5, 6]. Silicon nanowires or nanopillars have been shown to deform in a ductile way, unlike bulk material, with elasticity limits close to theoretical strength [7]. These phenomena are still the focus of an intense research activity, partly due to the development of dedicated nanomechanical testing [8].

Pioneering results on mechanical properties of SiNP mainly focused on crystalline nanospheres [8, 9], and reveal completely different behaviors compared to bulk materials. For instance, it was shown that small SiNP could plastically deform at room temperature [10], with very high yield stresses [11]. Other studies also revealed a toughness enhancement in SiNP [12]. Finally, maybe the most interesting aspect is that many plasticity mechanisms have been identified in SiNP, among which amorphization [13], dislocation nucleation and propagation [14, 15, 16, 17], and phase change [14, 16, 18, 19, 20]. Furthermore, not only the size but also the SiNP shape is shown to influence mechanical properties [21].

Another possible consequence of dimension reduction concerns the structure of the nanoparticle. In fact, the stability of certain phases could be enhanced in nanoparticles, although these are metastable in the bulk [22, 23, 24]. Furthermore, thermodynamics predict that for SiNP sizes below 3 nm, an amorphous state is favored [25]. Amorphous SiNP are important systems for high capacity Li-Si batteries [26, 27]. One of the main limitation for such applications is the large stress associated to lithiation, that could lead to cracks and limited charge–discharge cycling capabilities. It is therefore of paramount importance to fully characterize the mechanical properties of amorphous SiNP. However, there are apparently no reports on this specific topic in the scientific literature. To fill the gap, we investigate the behavior under compression of amorphous SiNP with sizes using atomistic calculations.

2 Simulation details

In this work, molecular dynamics (MD) simulations are carried out, both to generate and compress a-Si nanoparticles, using the LAMMPS code [28, 29]. A modified Stillinger-Weber potential represents the interatomic interactions [30].

Two SiNP sizes, corresponding to 10^5 and 10^6 atoms and hereinafter named as S (small) and L (large), are investigated. To generate the initial amorphous structure, the following procedure is adopted. Si atoms are first randomly introduced in a 80 Å sphere (150 Å) for the S (L) SiNP, into a supercell large enough to avoid interaction between periodic replicas. After an initial forces relaxation, the systems are heated to 3000 K with a ramp, then equilibrated at this temperature for 40 ps. The equations of motion are integrated with a 2 fs timestep. Next the temperature is lowered from 3000 K to 300 K in 54 ps, i.e. with a cooling rate of 5×10^{12} K s^{-1}. Surface atoms with a coordination lower than 2 are removed after this step. The systems are next equilibrated at 300 K for 40 ps. The final structures are used as starting configurations for the 300 K compression tests. An additional energy minimization is performed to produce initial configurations for the 5 K compression tests.

This procedure yields amorphous SiNP, approximately spherical in shape, with diameters of about 16 nm (34 nm) for the S (L) size. Five different structures are generated for each size. The analysis of the radial distribution functions reveals well relaxed disordered structures.

In a second step, the ten SiNP configurations are compressed according to the procedure depicted in [21], i.e. between two planar repulsive force fields moving towards each other at a constant velocity equal to 0.2 Å ps^{-1}, at temperatures of 300 K and 5 K. The simulation timestep for these simulations is now 1 fs. The true compression stress is obtained by first determining the numbers of Si atoms in "contact" with the indenters, using a 1 Å distance criterion, then by computing the contact surface area by Delaunay triangulation using all these atoms [21].

3 Results

The variations of calculated contact stresses during compression, averaged over five samples in each case, are represented in Fig. 1. Curves are overall similar, the stress increasing until 15–20% strain then slowly decreasing. Stress variations exhibit ripples, as the consequences of atomic reorganizations involving few atoms usually localized in the vicinity of the contact surfaces. This feature is also observed for crystalline SiNP [21], but is more pronounced here. At low strains, i.e. below 1%, the stress increase rates seem greater for S than for L systems in the figure, but examining stress variations

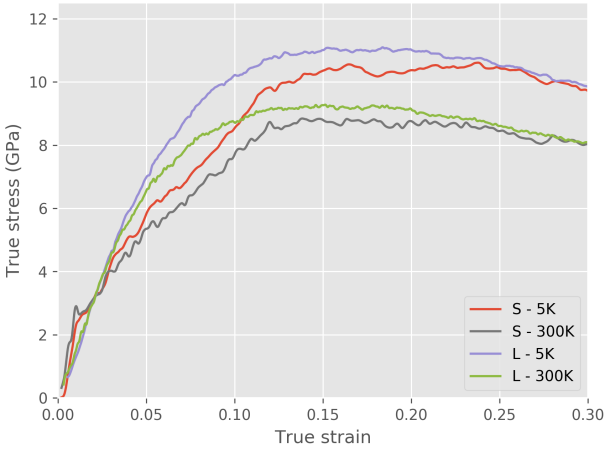

Fig. 1 Stress–strain curves associated to the compression of amorphous SiNP nanoparticles, averaged over 5 samples, for each case (S and L sizes, and respectively at 5 K and 300 K).

for each sample reveal a lot of dispersion in the results. However, at about 3%, there is a net slope change for S SiNP, observed for all samples, but not for L ones. The rationale for such behavior is not clear and requires further investigations.

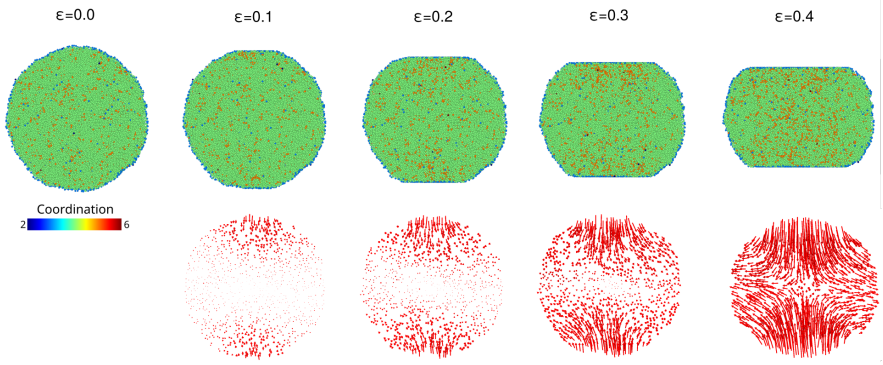

Fig. 2 Coordination numbers at different strains for the atoms at the center of a S SiNP at 5K (top row), as well as the cumulated atomic displacements with respect to the initial state for a random selection of the central atoms in the same SiNP (bottom row).

When strains exceed 5%, the stress increase tends to slow down. Examining the SiNP shape variation during compression (Fig. 2) reveals that it is partly due to the area increase of the surfaces contacting with the indenters.

Consequently, the initially spherical SiNP become barrel-like as compression is pursued. Furthermore, load continues to increase but with a decreasing rate.

Plastic deformation occurs for low strains, mainly by atomic rearrangements in the vicinity of the contact surfaces. These events are thermally activated, leading to more efficient stress relaxation at 300 K for both sizes, and thus a reduced stress increase compared to 5 K results. Maximum stresses are reached in the approximate strain range 0.12–0.24, with a larger plateau for S SiNP. Interestingly, for strains greater than 0.25, stresses for S and L systems become close, at both temperatures. This suggests that the flow stress depends on the temperature, but not on the SiNP size.

By analogy with experiments, we define the SiNP yield stress as the maximum attainable contact stress during compression. Taking into account all samples, the following values are determined: 11.0 ± 0.2 GPa for L at 5 K, 10.5 ± 0.7 GPa for S at 5 K, 9.2 ± 0.2 GPa for L at 300 K, and finally 8.5 ± 0.7 GPa for S at 300 K. Not surprisingly, higher yield stresses are found at low temperatures, with a difference of about 2 GPa between 5 K and 300 K tests. Also, large SiNP are characterized by higher values than the small ones. However, the difference is small, and there is a non negligible dispersion for S SiNP values.

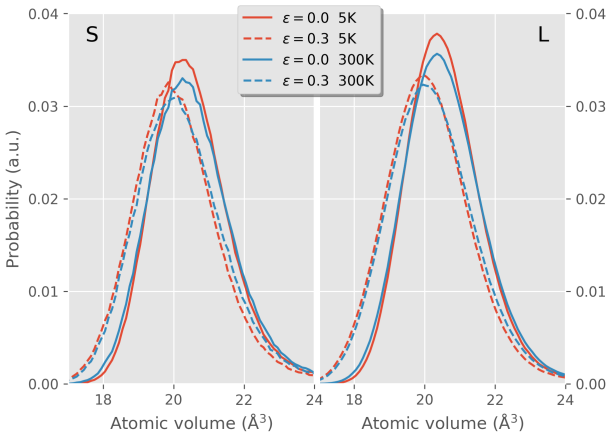

Fig. 3 Atomic Voronoi volume distributions for S (left) and L (right) SiNP, at 5 K and 300 K, before compression and at $\varepsilon = 0.3$.

From nanoindentation experiments on a-Si films, Gerbig et al. observed the formation of high-density a-Si or of the ordered β-tin phase, characterized by sixfold coordinated atoms, for contact stresses greater than 8.2 GPa [31]. In the present work, larger yield stress values are obtained in all cases. Therefore we analyze the atomic coordinations during compression, using a cutoff

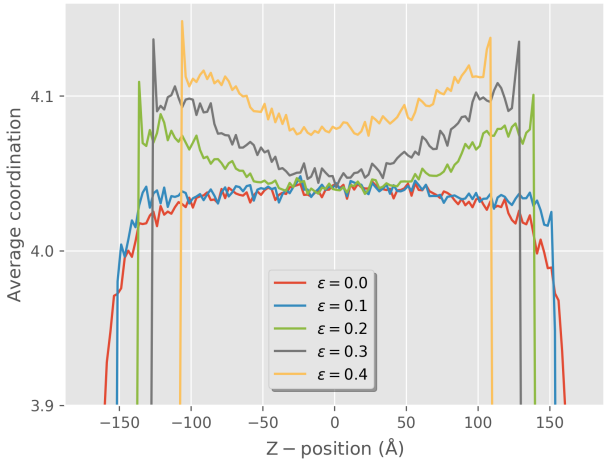

Fig. 4 Planar average of atomic coordination (Z-position origin at the center of the SiNP) along the compression axis, at different strains (L SiNP, 5 K).

radius of 2.85 Å [32]. Figure 2 shows coordination maps in a SiNP for different strains. A negligible amount of sixfold coordinated atoms is found, even at very high compression. Also, further structural analyses do not reveal the formation of β-tin regions. At last, the Fig. 3 shows the Voronoi volumes distributions in the unstrained SiNP and at 30%. We find that the compression only produces a weak densification of the SiNP, with about 2% volume reduction at 30%, regardless of temperature or SiNP size. Also there are no additional peaks at lower volumes in the distribution. These are further proofs that no high density a-Si phase or β-tin structure are formed during compression.

Figure 2 also shows the cumulated atomic displacements during compression. At low strains, only the atoms in the vicinity of the indenters are significantly displaced along the compression direction, in agreement with the stress localization predicted by Hertz theory. At 20% and higher strains, i.e. when contact stresses begin to decrease, these atoms become progressively pushed towards the free lateral surfaces of the SiNP. The lateral expansion during compression, explains why only a moderate densification is observed into the SiNP, conversely to a-Si films. This is similar to the deconfinement effect as suggested by Chrobak et al. for crystalline SiNP [33].

It is noteworthy that the amount of fivefold coordinated atoms seems to increase during compression, as suggested in Fig. 2. Such atoms are known to be "plasticity carriers" in the plastic deformation of bulk a-Si [34, 35]. Also, regions with highest concentrations appear to contain atoms with the largest atomic displacements. To confirm this point, we plot the planar average of atomic coordinations along the compression axis at different compression

states (Fig. 4). A clear increase of fivefold atoms is observed between 10% and 20%, i.e. for maximum contact stresses, in regions close to the indenters. At higher strains, their number continues to grow, especially in the center of the SiNP. This suggests an overt correlation between fivefold atoms and the plastic flow during compression.

4 Conclusions

Our investigations provide several original conclusions. First, we find no evidence of a significant size effect, a result similar to the one obtained for crystalline SiNP of similar sizes. However, more than two sizes should be investigated for definite conclusions. Another result is the prediction that the flow stress at high strains depends only on temperature, but not on size, confirming stress relaxation by thermally activated localized plasticity mechanism. The latter are associated to the formation of fivefold coordinated atoms, first in the vicinity of the indenters at about 10–20% deformation, then everywhere in the SiNP at high compression. This is related to the atomic displacements during compression, atoms close to the indenters being first pushed towards the SiNP center. At a later stage, it becomes favorable for these atoms to move laterally in the direction of the free SiNP surfaces. This mechanism allows to relieve the pressure exerted by the indenters, and leads to the barrel-like shape of the compressed SiNP. It is of interest to point that the plastic deformation of the SiNP is different from what is known in bulk a-Si [36, 37]. In fact, here the stress field imposed by the indenters is highly inhomogeneous, and drives the localization and activation of plastic events. Also, compared to indentation of a-Si bulk or films, the plastic deformation is not confined, preventing the formation of high density phases.

References

1. Zhenhui Kang, Yang Liu, and Shuit-Tong Lee. Small-sized silicon nanoparticles: new nanolights and nanocatalysts. *Nanoscale*, 3:777–791, 2011.
2. Maziar Ashuri, Qianran He, and Leon L. Shaw. Silicon as a potential anode material for li-ion batteries: where size, geometry and structure matter. *Nanoscale*, 8:74–103, 2016.
3. Minseong Ko, Sujong Chae, Sookyung Jeong, Pilgun Oh, and Jaephil Cho. Elastic a-silicon nanoparticle backboned graphene hybrid as a self-compacting anode for high-rate lithium ion batteries. *ACS Nano*, 8(8):8591–8599, 2014.
4. S. Öğüt, J. R. Chelikowsky, and S. G. Louie. Quantum confinement and optical gaps in si nanocrystals. *Phys. Rev. Lett.*, 79(9):1770, 1997.
5. M. D. Uchic, D. M. Dinmiduk, J. N. Florando, and W. D. Nix. Sample dimensions influence strength and crystal plasticity. *Science*, 305:986, 2004.

6. Julia R. Greer and Jeff Th.M. De Hosson. Plasticity in small-sized metallic systems: Intrinsic versus extrinsic size effect. *Progress in Materials Science*, 56(6):654 – 724, 2011.
7. Fredrik Östlund, Karolina Rzepiejewska-Malyska, Klaus Leifer, Lucas M. Hale, Yuye Tang, Roberto Ballarini, William W. Gerberich, and Johann Michler. Nanostructure fracturing: Brittle-to-ductile transition in uniaxial compression of silicon pillars at room temperature. *Adv. Funct. Materials*, 19(15):2439–2444, 2009.
8. Julia Deneen, WilliamM. Mook, Andrew Minor, WilliamW. Gerberich, and C. Barry Carter. In situ deformation of silicon nanospheres. *J. Mater. Sci.*, 41(14):4477–4483, 2006.
9. W. M. Mook, J. D. Nowak, C. R. Perrey, C. B. Carter, R. Mukherjee, S. L. Girshick, P. H. McMurry, and W. W. Gerberich. Compressive stress effects on nanoparticle modulus and fracture. *Phys. Rev. B*, 75:214112, Jun 2007.
10. William W. Gerberich, Douglas D. Stauffer, Aaron R. Beaber, and Natalia I. Tymiak. A brittleness transition in silicon due to scale. *J. Mater. Research*, 27:552–561, 2 2012.
11. W.W Gerberich, W.M Mook, C.R Perrey, C.B Carter, M.I Baskes, R Mukherjee, A Gidwani, J Heberlein, P.H McMurry, and S.L Girshick. Superhard silicon nanospheres. *J. Mech. Phys. Solids*, 51(6):979 – 992, 2003.
12. A.R. Beaber, J.D. Nowak, O. Ugurlu, W.M. Mook, S.L. Girshick, R. Ballarini, and W.W. Gerberich. Smaller is tougher. *Philos. Mag.*, 91(7-9):1179–1189, 2011.
13. Kuan-Chuan Fang, Cheng-I Weng, and Shin-Pon Ju. An investigation into the mechanical properties of silicon nanoparticles using molecular dynamics simulations with parallel computing. *J. Nanopart. Res.*, 11(3):581–588, 2009.
14. Ning Zhang, Qian Deng, Yu Hong, Liming Xiong, Shi Li, Matthew Strasberg, Weiqi Yin, Yongjie Zou, Curtis R. Taylor, Gregory Sawyer, and Youping Chen. Deformation mechanisms in silicon nanoparticles. *J. Appl. Phys.*, 109(6):063534, 2011.
15. L.M. Hale, D.-B. Zhang, X. Zhou, J.A. Zimmerman, N.R. Moody, T. Dumitrica, R. Ballarini, and W.W. Gerberich. Dislocation morphology and nucleation within compressed si nanospheres: A molecular dynamics study. *Comp. Mat. Sci.*, 54(0):280 – 286, 2012.
16. Andrew J. Wagner, Eric D. Hintsala, Prashant Kumar, William W. Gerberich, and K. Andre Mkhoyan. Mechanisms of plasticity in near-theoretical strength sub-100 nm si nanocubes. *Acta Mater.*, 100:256 – 265, 2015.
17. L. Yang, J. J. Bian, H. Zhang, X. R. Niu, and G. F. Wang. Size-dependent deformation mechanisms in hollow silicon nanoparticles. *AIP Advances*, 5(7):077162, 2015.
18. P. Valentini, W. W. Gerberich, and T. Dumitrică. Phase-transition plasticity response in uniaxially compressed silicon nanospheres. *Phys. Rev. Lett.*, 99:175701, Oct 2007.
19. L.M. Hale, X. Zhou, J.A. Zimmerman, N.R. Moody, R. Ballarini, and W.W. Gerberich. Phase transformations, dislocations and hardening behavior in uniaxially compressed silicon nanospheres. *Comp. Mat. Sci.*, 50(5):1651 – 1660, 2011.
20. Yu Hong, Ning Zhang, and Mohsen Asle Zaeem. Metastable phase transformation and deformation twinning induced hardening-stiffening mechanism in compression of silicon nanoparticles. *Acta Mater.*, 145:8 – 18, 2018.
21. D. Kilymis, C. Gérard, J. Amodeo, U.V. Waghmare, and L. Pizzagalli. Uniaxial compression of silicon nanoparticles: An atomistic study on the shape and size effects. *Acta Mater.*, 158:155–166, oct 2018.
22. S. H. Tolbert, A. B. Herhold, L. E. Brus, and A. P. Alivisatos. Pressure-induced structural transformations in si nanocrystals: Surface and shape effects. *Phys. Rev. Lett.*, 76(23):4384, 1996.
23. C.-C. Chen, A. B. Herhold, C. S. Johnson, and A. P. Alivisatos. Size dependence of structural metastability in semiconductor nanocrystals. *Science*, 276:398, 1997.
24. S. Illy, O. Tillement, F. Machizaud, J. M. Dubois, F. Massicot, Y. Fort, and J. Ghanbaja. First direct evidence of size-dependent structural transition in nanosized nickel particles. *Philos. Mag. A*, 79(5):1021, 1999.

25. S. Vepřek, Z. Iqbal, and F.-A. Sarott. A thermodynamic criterion of the crystalline-to-amorphous transition in silicon. *Philos. Mag. B*, 45(1):137, 1982.
26. Matthew T. McDowell, Seok Woo Lee, Justin T. Harris, Brian A. Korgel, Chongmin Wang, William D. Nix, and Yi Cui. In situ tem of two-phase lithiation of amorphous silicon nanospheres. *Nanoletters*, 13(2):758–764, 2013.
27. Andreas Pedersen, Michael Bieri, Mathieu Luisier, and Laurent Pizzagalli. Lithiation of silicon nanoclusters. *Phys. Rev. Applied*, 7:054012, May 2017.
28. http://lammps.sandia.gov/.
29. Steve Plimpton. Fast parallel algorithms for short-range molecular dynamics. *J. Comput. Phys.*, 117(1):1 – 19, 1995.
30. L Pizzagalli, J Godet, J Guénolé, S Brochard, E Holmstrom, K Nordlund, and T Albaret. A new parametrization of the stillingerweber potential for an improved description of defects and plasticity of silicon. *Journal of Physics: Condensed Matter*, 25(5):055801, 2013.
31. Y. B. Gerbig, C. A. Michaels, J. E. Bradby, B. Haberl, and R. F. Cook. In situ spectroscopic study of the plastic deformation of amorphous silicon under nonhydrostatic conditions induced by indentation. *Phys. Rev. B*, 92(21), dec 2015.
32. Andreas Pedersen, Laurent Pizzagalli, and Hannes Jnsson. Optimal atomic structure of amorphous silicon obtained from density functional theory calculations. *New Journal of Physics*, 19(6):063018, 2017.
33. D. Chrobak, N. Tymiak, A. Beaber, O. Ugurlu, W.W. Gerberich, and R. Nowak. Deconfinement leads to changes in the nanoscale plasticity of silicon. *Nature Nanotechnology*, 6:480, 2011.
34. Michael J. Demkowicz and Ali S. Argon. Liquidlike atomic environments act as plasticity carriers in amorphous silicon. *Phys. Rev. B*, 72(24), dec 2005.
35. M. Talati, T. Albaret, and A. Tanguy. Atomistic simulations of elastic and plastic properties in amorphous silicon. *Europhys. Lett.*, 86:66005, 2009.
36. C. Fusco, T. Albaret, and A. Tanguy. The role of local order in the small-scale plasticity of model amorphous materials. *Phys. Rev. E*, 82:066116, 2010.
37. Ali Kerrache, Normand Mousseau, and Laurent J. Lewis. Amorphous silicon under mechanical shear deformations: Shear velocity and temperature effects. *Phys. Rev. B*, 83(13), apr 2011.